Evolutionary Biology
https://doi.org/10.1007/s11692-020-09525-7

RESEARCH ARTICLE

Unlinking the Speciation Steps: Geographical Factors Drive Changes in Sexual Signals of an Amazonian Nurse-Frog Through Body Size Variation

Igor Yuri Fernandes[1] · Leandro J. C. L. Moraes[2] · Marcelo Menin[3] · Izeni Pires Farias[4] · Albertina Pimentel Lima[1,2] · Igor Luis Kaefer[1,3]

Received: 19 March 2020 / Accepted: 11 December 2020

Abstract

Geographical and environmental distances influence the divergence of characters among biological populations, especially on a macro spatial scale, making it difficult to interpret the individual contribution of these predictor variables in the process of population differentiation. Anurans are excellent models for multi-character evolutionary studies, due to their low vagility and frequent territoriality, causing certain environmental changes to result in barriers that isolate populations. Accordingly, we propose to test the correlation of environmental and geographical distances in the absence of obvious vicariant barriers with phenotypic and genotypic population characters using, as a study model, an Amazonian litter-frog (*Allobates sumtuosus*). Combining univariate and multivariate analyses, and Structural Equation Modeling, we tested the general hypotheses that geographical and environmental distances affect the variation in the morphometric, acoustic and genetic characters of this frog along a latitudinal gradient at a fine spatial scale. We found that the latitudinal variation was the most correlated with the variation of the studied characters, with an explanatory force always greater than 78%. Therefore, we suggest that there is a combined effect of latitude and environment on phenotypic characteristics in *A. sumtuosus*. These factors shape the acoustic characters of this species through pressures on body size, as confirmed by a regression analysis showing that larger body sizes resulted in lower-spectral frequency acoustic signals. This is because the climatic environmental gradient occupied by the species promotes changes in the area-volume relationship of individuals, resulting in larger body sizes towards the Equator. Although we observed a pronounced intrapopulation genetic structure, it was not associated with phenotypic variation. In summary, our study breaks down the stages of speciation for this Amazonian litter-frog, demonstrating that environmental factors lead to changes in the sexual signal due to the variation in body size.

Keywords Amazonia · Anura · Biogeography · Genotype · Landscape · Phenotype

Introduction

Intraspecific diversification is highly influenced by landscape factors, such as environmental heterogeneity and vicariant barriers to gene flow (Leão-Pires et al., 2018; Maia-Carvalho et al., 2018). The role of the landscape as

---

Supplementary Information The online version contains supplementary material available at https://doi.org/10.1007/s11692-020-09525-7.

✉ Igor Yuri Fernandes
igor.crotalus@hotmail.com

[1] Programa de Pós-Graduaçãoção Em Ecologia, Instituto Nacional de Pesquisas da Amazônia, Av. André Araújo 2936, Petrópolis, Manaus, AM 69067-375, Brazil

[2] Coordenação de Biodiversidade, Instituto Nacional de Pesquisas da Amazônia, Av. André Araújo 2936, Petrópolis, Manaus, AM 69067-375, Brazil

[3] Departamento de Biologia, Instituto de Ciências Biológicas, Universidade Federal do Amazonas, Av. General Rodrigo Octávio, 6200, Coroado I, Manaus, AM 69080-900, Brazil

[4] Laboratório de Evolução e Genética Animal, Departamento de Genética, Instituto de Ciências Biológicas, Universidade Federal do Amazonas, Av. General Rodrigo Octávio, 6200, Coroado I, Manaus, AM 69080-900, Brazil

an inducer of population differences, which can lead to speciation, and thus affect species composition of local assemblages, has been widely tested in tropical regions (Morales-Jimenez et al., 2015; Dal Vechio et al., 2018; Naka & Brumfield, 2018; Ribas et al., 2018). Both the adaptive capacity of organisms and genetic drift can result in phenotypic and genotypic differentiations between populations, which may experience restriction or even interruption of gene flow, leading to the formation of new species (Tryjanowski et al., 2006; Cortázar-Chinarro et al., 2017; van Rensburg et al., 2018). In addition, the stages of differentiation of classes of genotypic and phenotypic characters do not obey a fixed order during the process of lineage separation, so that the sequence of appearance of evolutionary novelties is essentially idiosyncratic (De Queiroz, 2007). In this context, multi-character studies addressing differentiation among populations across continuous landscapes (i.e. in the absence of biogeographical barriers or abrupt environmental changes) are still scarce.

Both geographic distance and environmental variation influence the character divergences among biological populations. Usually, these factors co-vary, especially when analyzed at a macro-spatial scale, making it difficult to interpret their individual contributions as predictor variables in the population differentiation process (Kaefer et al., 2013; Maia et al., 2017). Thus, understanding the effect of such factors on multiple character classes at local or regional spatial scales helps clarify the role of the landscape variation in the evolution of genetic and phenotypic traits of populations (Mullen et al., 2009; Spurgin et al., 2014; Valenzuela-Sánchez et al., 2015).

Anuran are excellent models for multi-character evolutionary studies, since their low vagility and frequent territoriality, associated with a short generation time (Zimmerman & Bierregaard, 1986; Ernst & Rödel, 2008; Menin et al., 2007; Keller et al., 2009), tend to generate well-marked spatial and environmental variation in their phenotypic and genotypic characteristics. Several studies at finer spatial scales demonstrate that anuran populations tend to be highly-structured genetically, with gene flow decreasing as the geographical distance between these populations increases (Newman & Squire, 2001; Lampert et al., 2003; Marchesini et al., 2017; Kobayashi et al., 2018). This is intensified by the fact that anuran generally have spatially restricted reproductive sites, causing environmental variation to act as often insurmountable barriers for individuals, further isolating populations (Kobayashi et al., 2018). However, few studies have tested how phenotypic and genotypic changes in anurans occur in relation to geographical and environmental distances, and often the landscape is simply treated categorically (Kaefer & Lima, 2012; Maia et al., 2017; Ortiz et al., 2018).

In addition, anurans are suitable for integrative studies because they recognize, and selectively reproduce, through acoustic signals (Beebee, 2005; Zeisset & Beebee, 2008). Call characteristics in these organisms are generally allometrically linked to their body size (Hoskin et al., 2009; Gingras et al., 2013), because spectral features are affected by the size of the organs involved in producing vocalizations (*e.g.* mass of vocal cords, laryngial musculature) which are, in turn, correlated with body size (Martin, 1972; Jaramillo et al., 1997). It is known that the relationship between body size and call frequency is negative: individuals or species with larger body sizes tend to call at lower frequencies (Gingras et al., 2013). Differences in the acoustic signals can affect the recognition limits in the acoustic space (Amézquita et al., 2011). Thus, the lack of recognition or selection of the male's sexual signal by the female can lead to speciation processes via the formation of a pre-zygotic reproductive barrier (Boul et al., 2007).

Structural (*e.g.* vegetation and soil) and climatic (*e.g.* temperature and precipitation) environmental factors act directly on the occurrence and abundance of Amazonian anurans, potentially facilitating or restricting interpopulation gene flow (Maia et al., 2017; Ortiz et al., 2018; Ferreira et al., 2018, 2020). Environmental heterogeneity along latitudinal gradients can affect the body length of frogs, with variation in temperature and precipitation being the main regulators of this character, since they control important life-history features as reproductive season duration and prey availability (Ficetola & Maiorano, 2016). Additionally, populations of frogs that occupy environments with greater temperature seasonality have a larger average body size (Valenzuela-Sánchez et al., 2015).

Allobates sumtuosus (Morales, 2002) (Anura, Dendrobatoidea, Aromobatidae) is a terrestrial and diurnal Amazonian litter-frog, which mainly reproduces at the peak of the rainy season, as is common for members of the genus (Simões & Lima, 2012; Simões et al., 2013). In the reproductive period, males vocalize in the vicinity of isolated puddles, mainly in riparian environments (Jorge et al., 2016). The species is a good model for multi-character evolutionary studies because of its functional characteristics, including small size, reproduction with egg deposition in leaf litter, and high level of male territoriality, which have small home ranges, as well as occurring in a larger area that involves latitudinal environmental gradients (Simões et al., 2013). Such characteristics are known to reduce individual dispersion and promote molecular and/or phenotypic differentiation in the face of physical or environmental barriers (Moraes et al., 2016), and so are appropriate characteristics for studies involving historical and ecological biogeography.

Accordingly, we propose to test the correlation of environmental and latitudinal distances with the variation on phenotypic and genotypic characters using populations of *A. sumtuosus* as study models in a spatial context with no evident vicariant barriers. Our main objective is to test the general hypotheses that latitudinal and environmental variation affect the morphometric, acoustic and genetic differentiation of *A. sumtuosus* along a gradient at a fine spatial scale. Our predictions are: (1) latitudinal and environmental variation will be correlated with differentiation in body size, which should be negatively related to the frequency of acoustic signals; (2) an increase in genetic distances between sampled populations will imply in an increase in respective phenotypic distances (estimated from body size and frequency of acoustic signal).

Material and Methods

Study Area

This study was carried out along a Amazonian latitudinal gradient, composed of sampling localities in the northern and southern hemispheres, in the Brazilian states of Amazonas and Roraima (Fig. 1, Table 1). The vegetation matrix that covers the sampling area, as well as most of the latitudinal segment, is the lowland humid tropical forest, characterized by a closed canopy and a dense understory with abundant palm trees (Ribeiro et al., 1999). According to the climate classification, sampling area vegetation types is composed of the Af domain (tropical rainforest) in the southern hemisphere, and the Am domain (tropical monsoon) in the northern hemisphere. The rainy season in the southern hemisphere extends from December to March, while in the northern hemisphere the rain peak is in mid-June to July. Fieldwork was conducted from January to July 2019, in the morning (05: 30–11: 00 h), peak time of vocal activity of the focal species (Juncá, 1998).

Morphological Data

Collected individuals (five or seven males by each locality, total = 65) were euthanized by applying a topical anesthetic (5% benzocaine) (under permission granted by Instituto Chico Mendes de Conservação da Biodiversidade (ICMBio) number 67501-2) on their ventral surfaces, labeled, fixed in 10% formaldehyde, and then preserved in 70% ethanol and deposited in the Amphibian and Reptile Collection of the Brazilian National Institute for Amazonian Research (See Supplementary Material). With a Leica stereomicroscope (model S8APO) coupled to a Leica DFC295 camera, 23 morphometric measurements were obtained with a precision of 0.001 mm (except for SVL, which was measured with digital calipers at a precision of 0.01 mm), following Simões et al. (2013): snout-to-vent length (SVL), length of the head from the tip of the snout to the posterior edge of the maxillary joint (HW), width of the head at the level of the maxillary joint (HL), length from the tip of the snout to the anterior margin of the eye (SL), eye-nostril distance from the anterior margin of the eye to the center of the nostril (EN), internarial distance taken by the outer margins (IN), eye length from the anterior to the posterior margin (EL), interorbital distance by the edges of the eyes on the dorsal

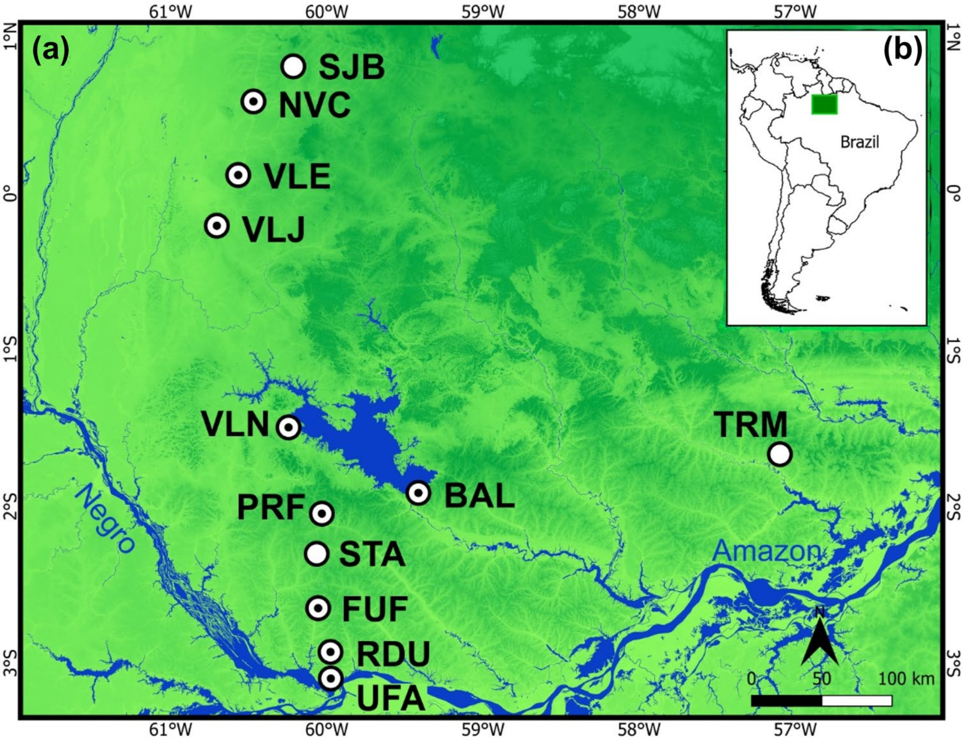

Fig. 1 Geographical distribution of *Allobates sumtuosus* study sampling sites (**a**) in northern South America (**b**). Black-dotted symbols indicate localities with associated morphology, acoustic and genetic data, and hollow symbols indicate localities represented only with genetic data. See Table 1 for population acronyms

Table 1 Locations sampled along the BR-174 highway, their respective acronyms used throughout the text, and number of samples obtained for the different sources of evolutionary data

Locality	Acronym	Coordinates	Morphology	Acoustic	mtDNA	
					NG	GB
Rio Trombetas (PA)	TRM	01°22′12"S, 56°51′08"W	–	–	–	4
Universidade Federal do Amazonas (AM)	UFA	03°06′0.85"S, 59°58′18.98"W	8	8	5	10
Reserva Florestal Adolpho Ducke (AM)	RDU	02°55′50.34"S, 59°58′28.68"W	8	8	5	3
Fazenda Experimental da UFAM (AM)	FUF	02°38′51.36"S, 60°03′13.43"W	7	7	6	18
Sítio Tamaga (AM)	STA	02°13′23"S, 60°03′55"W	–	–	–	1
Presidente Figueiredo (AM)	PRF	02°02′31.95"S, 60°01′46.98"W	7	7	5	–
Vila de Balbina (AM)	BAL	01°54′03.47"S, 59°24′52.12"W	7	7	4	–
Ramal Vila Nova—km 1062 (AM)	VLN	01°29′36.64"S, 60°14′25.12"W	7	7	4	–
Vila de Jundiá (RR)	VLJ	00°12′20.76"S, 60°41′46.54"W	7	7	6	–
Vila do Equador (RR)	VLE	00°07′24.93"N, 60°33′43.69"W	7	7	3	–
Nova Colina (RR)	NVC	00°34′55.23"N, 60°27′53.01"W	7	7	1	–
São João da Baliza (RR)	SJB	00°57′10"N, 59°55′43"W	–	–	–	2
		Total	**65**	**65**	**77**	

(Brazilian states: (AM) Amazonas; (PA) Pará; (RR) Roraima. Molecular data: (NG) newly generated sequences, directly associated with morphological and acoustic data; (GB) sequences downloaded from GenBank)

surface (IO), diameter of the tympanum from the anterior to the posterior margin (TYM), length of the forearm from the proximal edge of the palmar tubercle to the outer edge of the flexed elbow (FAL), length of the arm from the arm insertion to the outer edge of the flexed elbow (UAL), lengths from the proximal edge of the palmar tubercle to fingertips I, II, III and IV (respectively HAND I, HAND II, HAND III, HAND IV), width of the disc on finger III (WFD), width of the third phalanx of finger III (WPF), maximum diameter of the palmar tubercle (DTP), maximum diameter of the thenar tubercle (DTT), leg length from the posterior end of the coccyx to the outer edge of the flexed knee (LL), tibia length from the outer edge of the knee to the flexed heel (TL), foot length from the proximal edge of the external metatarsal tubercle to the tip of the toe IV (FL) and width of the disc on toe IV (WTD).

Acoustic Data

Vocalizations of all of the 65 aforementioned collected individuals were recorded for 3 min on average, using a Sony PCM—D50 digital recorder coupled to a Sennheiser ME66 directional microphone. Recordings were made approximately one meter distant from the individuals. Calls were analyzed using Raven Pro software, version 1.5 (Charif et al., 2010), where 10 notes were sampled, evenly distributed across the recording time (Simões et al., 2013). To do this, we divided the total number of notes in each recording by 10 and defined the resulting fraction as the sampling interval. For each recording, we measured the note duration (ND), peak frequency (NPF), lowest frequency (NLF) and highest frequency (NHF). Spectral analyzes were performed with a frequency resolution of 82 Hz and 2048 points, using the Blackman window format (Kaefer & Lima, 2012). Frequencies emitted by the notes were measured 20 dB below the peak frequency, as this represents the lowest point at which the energy transmitted by vocalization is distinguishable from background noise during recordings (Erdtmann and Amézquita, 2009). The air temperature was measured during each recording.

Genetic Data

Muscle tissue samples of specimens were obtained from the thighs of 39 representative individuals before fixation and preserved in absolute ethanol. Extraction and isolation of genomic DNA followed the salt extraction protocol with a final volume of 50 µL (Aljanabi & Martinez, 1997). The extraction product was quantified in NanoDrop (Applied Biosystems, Waltham, MA, USA) using the Nucleic Acid program, to verify the concentration of DNA (µg/ml) and impurities (proteins and carbohydrates remaining in the cell digestion process). Using polymerase chain reactions (PCR), the 16S region of the mitochondrial DNA was amplified with the primers 16Sar/16Sbr (Palumbi, 1996). This gene was selected due to its extensive use in studies of amphibian taxonomy and phylogeography, showing satisfactory inter- and intraspecific resolution (Vences et al., 2005; Fouquet et al., 2007). The PCR reaction material contained 4.4 µL of distilled and deionized water; 2.0 µL dNTPs; 2.3 µL MgCl; 1.5 µL of Tris–HCl buffer; 0.3 µL of BSA; 1.5 µL of each primer; 0.5 µL of Taq DNA polymerase and 1 µL of DNA.

The thermocycling process was performed according to the following steps: initial DNA strand denaturation at 92 °C for 30 s; 35 denaturation cycles at 92 °C for 10 s, annealing primers to the DNA strand at 50 °C for 35 s, extension of the new free nucleotide strands and fragments at 72 °C for 90 s and final extension at 72 °C for 10 min. PCR products were purified by reaction with EXO-SAP, following the protocol suggested by the manufacturer (Applied Biosystems, Waltham, MA, USA). For sequencing reactions we use the Big Dye Terminator sequencing kit (Applied Biosystems, Waltham, MA, USA), following the manufacturer's instructions. Sequenced products were precipitated in EDTA/ethanol and analyzed in an ABI3500 automatic capillary sequencer (Applied Biosystems, Waltham, MA, USA). All procedures were performed at the Laboratory of Animal Evolution and Genetics (LEGAL), at the Federal University of Amazonas (UFAM), Manaus, Amazonas, Brazil.

The newly generated sequences, with fragment size varying between 179 and 470 base pairs (bp) were edited and inspected in the Geneious Prime v.2.3 (Kearse et al., 2012). We complemented the molecular dataset by downloading 38 homologous sequences of the species with precise locality information deposited in the GenBank online repository, including samples from the species' type locality (fragment size varying between 350 bp and 470 bp). To align the final dataset with 77 sequences, we used the MAFFT 7 online (Katoh et al., 2019) under default parameters, except for the use of the E-INS-i strategy, best suited for genes with multiple conserved domains and long gaps (Katoh & Standley, 2013). The newly generated sequences were deposited in GenBank (see Supplementary Material for accession numbers).

Phylogenetic and Phylogeographic Analyzes

We reconstructed phylogenetic trees using both Bayesian Inference and Maximum Likelihood. The GTR + G nucleotide substitution model was selected as the most suitable for molecular data according to the PartitionFinder 2.1.1 program (Lanfear et al., 2017) under Akaike's corrected information criterion (AICc; Hurvich & Tsai, 1991). Sequences of *Allobates* species most closely related to *A. sumtuosus* (*A. bacurau* and *A. paleovarzensis*) were selected as external groups for analyses and obtained from GenBank. For the Bayesian analysis, in the MrBayes 3.2.6 program (Ronquist et al., 2012), we conducted four independent runs of 5 million generations, starting with random trees and four Markov chains, sampled every 1000 generations, discarding 25% of generations and trees as burn-in. Parameter convergence (Estimated Sample Size, ESS > 200) was assessed using the Tracer 1.7 program (Rambaut et al., 2018). Maximum Likelihood analysis was conducted with the RaxML 8.2.10 program (Stamatakis, 2014), researching the most likely tree 100 times and with support assessed through 1000 non-parametric bootstrap repetitions.

The most likely number of genetic clusters formed by the sampled mtDNA sequences was inferred through a Bayesian analysis of population structure using the BAPS v.6 program (Corander et al., 2008). Based on the nucleotide frequencies, this model seeks to generate groups of individuals, so that those assigned to the same group are as genetically similar to each other as possible. We executed the mixture model with a range of 2–10 k and four replicates. The result of this model was used to run the admixture model (Corander & Marttinen, 2006) using 100 iterations, 200 reference individuals and 10 iterations per individual. Values of $p < 0.05$ were considered significant evidence of admixture. To visualize the spatial structure among the sampled haplotypes, we built a haplotype network using the HaploView 4.2 program (Barrett et al., 2005), with the Maximum Likelihood tree topology. Lastly, we estimated the ΦST index of pairwise differentiation between the sampled populations using the *adegenet* package (Jombart, 2008) at the R environment (R Core Team, 2019).

Environmental Variables

We used three environmental variables to understand how the latitudinal environmental gradient affects the *A. sumtuosus* phenotype and genotype: (1) average annual thermal amplitude, which directly affects the amphibian immune system and can alter the susceptibility of these organisms to diseases (Raffel et al., 2006); (2) average annual precipitation, representing the relative humidity of the environment, which affects amphibians by maximizing or decreasing the rates of evaporation and loss of body water through their semipermeable skin (Mitchell and Bergmann, 2016); (3) percentage of sand in the soil, as more granular soils tend to retain less water and have more frequent saturation, which may affect the desiccation rate of *A. sumtuosus* eggs, which are deposited in leaflitter in locations with predominantly sandy soil (Juo & Franzluebbers, 2003). In addition, the spatial occurrence of *A. sumtuosus* is related to the presence of water bodies that, in turn, are correlated with higher percentages of sand on its margins (Simões et al., 2013).

We obtained the variables of mean annual thermal amplitude (BIO7) and mean annual precipitation (BIO12) for the period 1950–2000 from the online WorldClim database (Hijmans et al., 2005). The percentage of sand in the soil at a depth of 15 cm was obtained from the SoilGrids database (Hengl et al., 2014). All raster files used were interpolated for 30 arc-sec (~ 1 km^2), cut on the R environment (R Core Team, 2019) using the *raster*, *sp* and *rgeos* packages and the *extend* and *crop* functions, with the data extracted using the *extract* function (Hijmans et al., 2015).

Statistical Analyses

In view of the multivariate nature of our data, we perform Principal Component Analysis (PCA) to reduce the dimensionality of the morphological, acoustic, genetic and environmental data separately. Considering the sexual dimorphism presented by *A. sumtuosus*, where females have larger body sizes than males (Simões et al., 2013), we use only data obtained from males for the analyses. The PCA was used to summarize multivariate datasets, which can be correlated with each other, in few axes containing the variation, allowing the use of the first axis (PCA1) containing the greatest variation in subsequent univariate analyzes. After obtaining the PCA1 for each analyzed dataset, we performed a Structural Equation Modeling (SEM) analysis using the *lavaan* package (Rosseel, 2012) in the R environment (R Core Team, 2019). The SEM investigates the relationship between latent and observed variables through regressions between models, as well as their covariations, allowing the simultaneous assessment of combined influences of multiple factors (Rosseel, 2012). To access the relationship between the body size and the frequency of the call, and the relationship between the frequency of the call and air temperature, and effect of the latitudinal gradient on spectral characters of the acoustic signal of *A. sumtuosus* also through a linear regression test. These analyses were also conducted on the R environment using the *vegan* package (R Core Team, 2019).

Results

Phylogenetic and Phylogeographic Relationships

Both phylogenetic inference approaches generated congruent gene trees considering the phylogenetic relationships of the analyzed sequences (Fig. 2). These analyzes recovered both the monophyly of *A. sumtuosus* (PP—posterior probability = 1.0, BS—bootstrap support = 100), and the presence of two reciprocally monophyletic subclades contained under this name. Such subclades are segregated by a genetic distance of ca. 3% and correspond to populations in the westernmost localities of the species distribution (Western clade; Roraima and Amazonas states) (PP = 0.9, BS = 80) and the population at the species' type locality in the region of Rio Trombetas (TRM, Pará state) (PP = 1.0, BS = 100). The genotypic distances found between these subclades are equivalent to some intraspecific distances observed for other species of *Allobates* (Kaefer et al., 2013; Maia et al., 2017). Considering the Western clade, despite their interrelationships receiving low support due to the high similarity between the sequences (maximum of 2% of genetic distance), a trend can be seen in the segregation of the sequences. Samples from northern populations of our sampling (SJB, NVC, VLE and VLJ, Roraima state) are divergent from the populations of central (VLN, Amazonas state) and southern (BAL, PDF, STA, FUF, RDU AND UFA, Amazonas state) localities, with the central population (VLN) being more genetically differentiated than those in the southern subgroup.

BAPS analysis resulted in the most likely number of genetic clusters (k) = 4, with no evidence of admixture, corresponding to the populations of: (1) Rio Trombetas (TRM, Pará state); (2) northern; (3) central; and (4) southern distribution of our sampling (Fig. 2). The obtained haplotypes network, corresponding to 13 different haplotypes, mirrored this result, with more subtle segregation between the northern (2) and southern (4) populations of the sample, and greater differentiation of those from the central population of our sampling (3—VLN) and from the Rio Trombetas (1—TRM) (Fig. 3). Results of the ΦST analysis demonstrate a high level of general genetic structuring between the populations (Table 2).

Correlation Between Environmental, Geographical, Phenotypic and Genetic

The SEM analysis showed different correlations between all datasets (Table 3, Fig. 4). We detected a higher number of correlations with the latitudinal variation, with explanatory force above 63% (absolute $R^2 > 0.63$, $p < 0.01$). Our analysis also indicated that the latitude can explain about 78% of the observed environmental variation ($R^2 = -0.78$, $p < 0.01$). Latitude was also the variable with the greatest explanatory force for phenotypic data: 88% of the morphological variation ($R^2 = 0.88$, $p < 0.01$) and 63% of the acoustic variation ($R^2 = 0.63$, $p < 0.01$). Conversely, latitudinal variation was not detected as related with genetic changes ($R^2 = -0.14$, $p > 0.05$), and the model did not find statistically significant relationships between the environmental, genotypic and phenotypic variables, with explanatory forces below 36% ($R^2 = 0.36$, $p > 0.05$). The variation in genetic data explained a low percentage (26%) of the morphological variation in our datasets ($R^2 = -0.26$, $p < 0.05$). The correlation between morphological and acoustic datasets showed no statistically significant relationship ($R^2 = 0.44$, $p > 0.05$). However, the linear regression comparing only the body size (SVL) and call frequency showed a statistically significant negative relationship ($R^2 = 0.3$; $p < 0.01$) (Fig. 5a). The linear regression comparing the call frequency and air temperature showed no statistically significant relationship ($R^2 = 0.05$; $p > 0.05$) (Fig. 5b). Lastly, the effect of the latitudinal gradient on the spectral characters of the acoustic signals correspond to 39% of the variation in the peak frequency ($R^2 = 0.35$; $p < 0.05$) (Fig. 5c).

Fig. 2 Bayesian phylogenetic tree of *Allobates sumtuosus* populations (at left) based on the variation of a fragment of mtDNA (16S), showing the two best supported subclades; and the result of population structure analysis (BAPS) (at right), showing the clusters recovered represented by distinct colors (k = 4). Newly sequenced specimens are highlighted in bold. Asterisks represent support values of Bayesian inference between 0.9 and 1.0 (above branches) and Maximum likelihood between 80 and 100 (below branches). Branch scale is indicated in number of substitutions per site

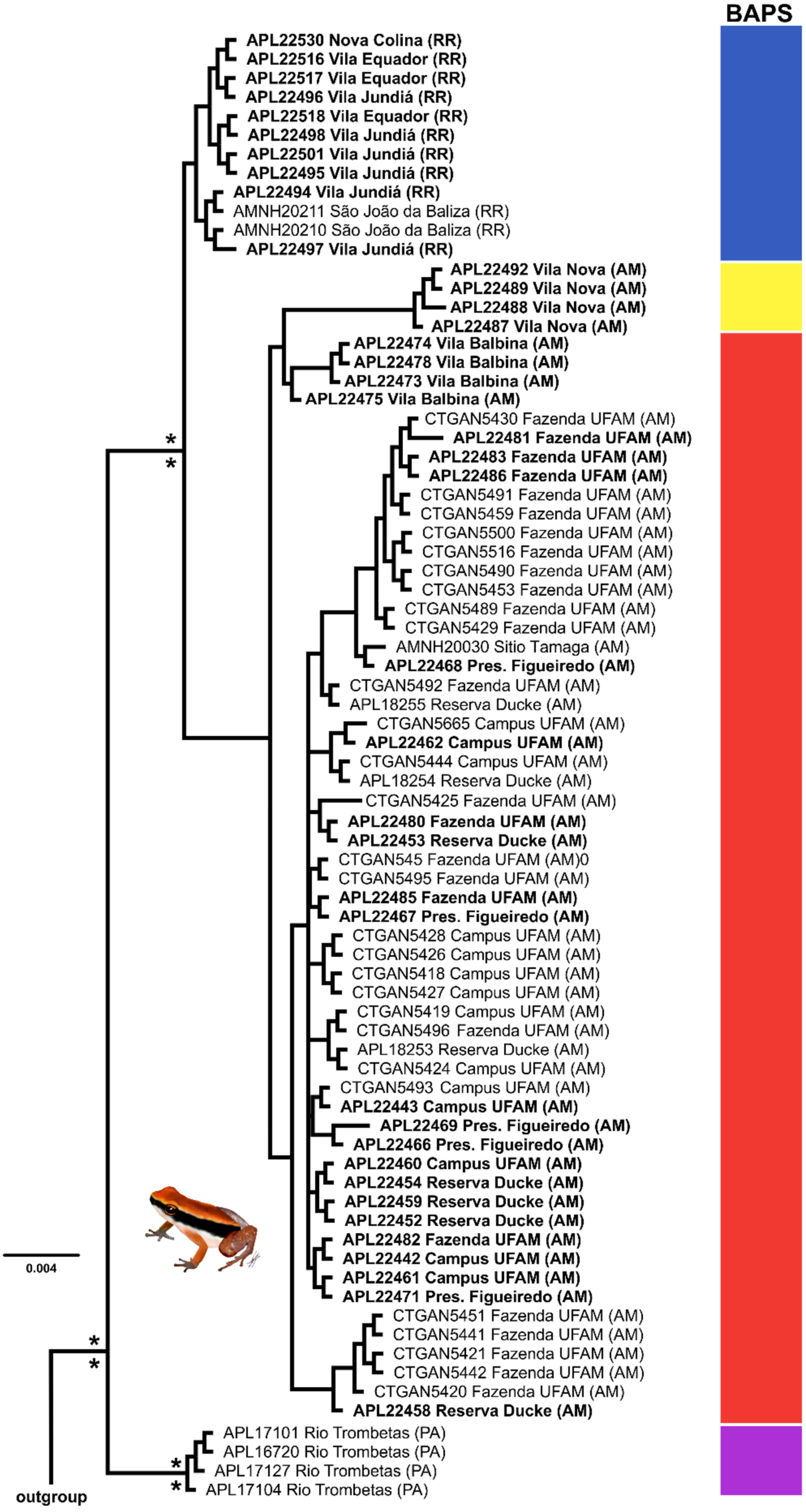

Fig. 3 Haplotype network (**a**) generated with 77 sequences of a fragment of the 16S mtDNA (179–470 base pairs) for *Allobates sumtuosus* and their geographic origin (**b**). The size of the circles in the network indicates the relative frequency of the haplotype and the color indicates the origin of the individuals corresponding to the geographic location in the sampled space (**b**). See Table 1 for population acronyms

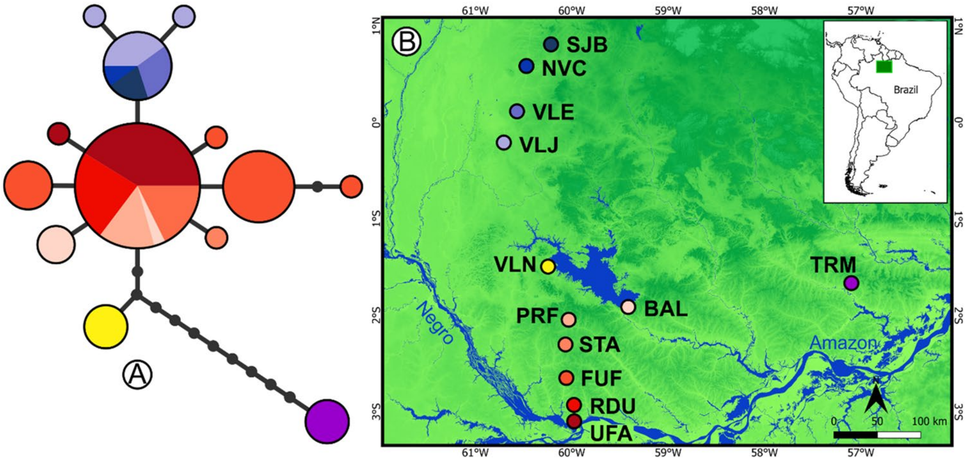

Table 2 Pairwise Φ_{ST} fixation indexes (upper right matrix) and average genetic distances (%) (lower left matrix)

Locality	UFA	RDU	FUF	PRF	BAL	VLN	VLJ	VLE	NVC
UFA	–	ID	0.271	0.167	0.711	1.000	0.878	1.000	1.000
RDU	0.0	–	0.158	0.043	0.631	1.000	0.83	1.000	1.000
FUF	0.3	0.3	–	0.118	0.46	0.715	0.569	0.547	0.484
PRF	0.2	0.2	0.5	–	0.496	0.788	0.606	0.619	0.539
BAL	0.4	0.4	0.8	0.6	–	0.838	0.625	0.666	0.623
VLN	1.1	1	1.3	1.3	1	–	0.929	1.000	1.000
VLJ	0.5	0.5	0.9	0.8	0.5	1.1	–	0.156	0.319
VLE	0.3	0.3	0.6	0.8	0.7	0.6	0.0	–	ID
NVC	0.4	0.6	0.4	0.9	1.1	0.4	0.1	0.2	–

Values calculated between the sampling localities of each *Allobates sumtuosus* population with associated morphological and acoustic data. See Table 1 for population acronyms

ID insufficient data

Table 3 Results of the Structural Equation Modeling (SEM) analysis, with regressions (variable 1 × variable 2), correlating the geographical and environmental distances with phenotypic and genetic variation of *Allobates sumtuosus* from the sampled locations

Model	R^2	p-value
Env ~ Lat	**−0.78**	**0.0002***
Mor ~ Lat	**0.88**	**0.00001***
Mor ~ Env	0.08	0.62
Mor ~ Gen	**−0.26**	**0.023***
Aco ~ Lat	0.63	0.12
Aco ~ Env	0.20	0.38
Aco ~ Mor	0.43	0.23
Gen ~ Lat	−0.14	0.76
Gen ~ Env	0.44	0.36

Statistically significant relations ($P \leq 0.05$) are highlighted in bold

Model variables abbreviations: *Lat* latitude, *Mor* morphology, *Aco* acoustic, *Gen* genetic, *Env* environment

Discussion

The results obtained by our SEM and regression analyzes clearly demonstrates a combined effect of latitude and environmental variation exerting selective pressures on the morphological and acoustic characteristics of *Allobates sumtuosus* populations. In fact, environmental variation given by physical or climatic factors are already recognized as one of the major drivers of phenotypic changes in vertebrates, as the phenotype connects the evolutionary process and the environment (Tryjanowski et al., 2006; Ng et al., 2013). Moreover, the strong relationship between latitude and the environment also show that when the inclusion of the latitude as a variable in the modeling somehow masked the environmental effects.

The environmental variation in the continuous landscape studied can be mainly a result of the recognized climatic gradient occurring along the latitudinal variation (Chu et al., 2019). At sampling localities closer to the Equator (VLJ, VLE and NVC), precipitation levels

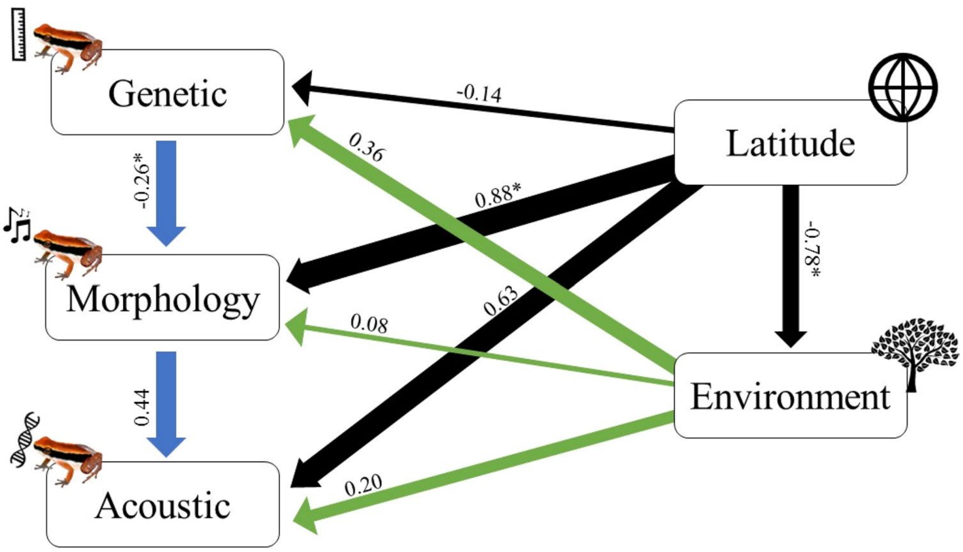

Fig. 4 Results of the correlations among each analyzed character class (genetic, morphology and acoustic) and predictor variables (environment and latitude), obtained through a Structural Equation Modeling analysis. The results for the tests for statistical significance of the correlations can be found in Table 3

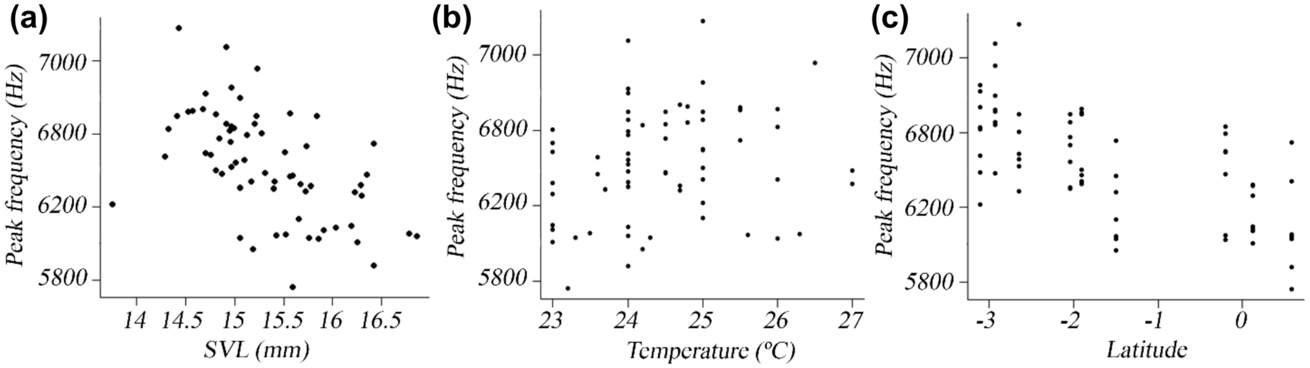

Fig. 5 Relationships between body size (snout–vent length; SVL), air temperature and latitude with the peak frequency of the advertisement call among sampled populations of *Allobates sumtuosus*

tend to be lower and average annual temperatures tend to be higher when compared to the southernmost sampling localities (Liberato & Brito, 2010). It is already known that these variables can directly affect the body size of frogs, via trade-offs caused by the relationship surface-volume of individuals (Mitchell and Bergmann, 2016). Larger body sizes have lower area-volume ratio and this is advantageous in warmer and relatively drier habitats, as it neutralizes the negative effect of water loss through evaporation from the skin, which in this case will be slowed down (Bevier et al., 2008; Mitchell and Bergmann, 2016). The development of larger bodies can be explained by factors such as the extended longevity of individuals, which, associated with a slower but constant growth rate, will lead to an increase in body volume (Liao and Lu, 2012; Liu et al., 2018). The environmental variation along the latitudinal gradient studied tend to provide selective pressures to amphibian body sizes, which can lead to the reported expression of greater body sizes in populations of *A. sumtuosus* closer to Equator. Our study was performed at a mesoscale spatial, but such results are also similar to that found in large-scale studies that addressed the effect of latitude on anuran morphology, showing a tendency to body size increase in populations closer to the warmer zone of Equator (Liu et al., 2018).

An intraspecific increase in the body size of frogs is also known to promote changes in their acoustic parameters, especially a general lowering on the frequency of the call (see Gingras et al., 2013 for an example at the interspecific level). This allometric relationship was corroborated in our studied populations of *A. sumtuosus*, as individuals with smaller body size from the southernmost sampling localities tended to generate acoustic signals with higher peak frequencies compared to individuals from northern sampling localities. The most striking differences were found when we compared the data of the population from a southern locality (RDU), with a mean peak frequency of the call of 6744 ± 336 Hz (6380–7080 Hz; n = 8), with population from a northern locality (NVC), whose peak frequency of calls reached a mean peak frequency of 6094 ± 246 Hz (5762–6546 Hz; n = 7). The interpopulational variation reported here for the *A. sumtuosus* call could also be influenced by the environmental variation, as the "acoustic adaptation hypothesis" proposes that the spectral parameters of the call tend to reach lower values in forest areas (or in denser forests), because lower frequencies generate a more effective propagation of the acoustic signal (Morton, 1975; Erdtmann & Lima, 2013). However, when both the morphological and acoustic variations are compared in a combined way to the environmental variation, it is evident that the morphology is the most affected characteristic (Bevier et al., 2008). Such results supports the interpretation that in our studied system, variation in acoustic signals of *A. sumtuosus* are mostly related to the morphological changes among populations, which in turn are related with the environmental variation through the latitudinal gradient.

In a study of the acoustic recognition space in dendrobatoids, Amézquita et al. (2011) showed that the maximum limiting acoustic ('acoustic space') for the genus *Allobates* is ca. 1000 Hz at the intraspecific level. The existence of the detected variation among calls of *A. sumtuosus* populations in our sampling area indicate that the populations at the extreme of acoustic divergence may be close to the limit of acoustic recognition at the intraspecific level. When we refined the results at an individual level, this postulated limit for intraspecific recognition was exceeded, as some individuals in the southern populations call at a peak frequency of 7181 Hz, while some individuals in the northern population call a peak frequency of 5762 Hz (difference = 1419 Hz). Thus, based on the results of Amézquita et al. (2011), we suggest that southernmost and northernmost populations at the sampled area would not acoustically recognize each other in case of secondary contact. Based on the fact that acoustic recognition is essential for the reproductive success of anurans (Boul et al., 2007) these divergent populations likely achieved the pre-zygotic isolation criterion according to the classic (biological) species delimitation model (de Queiroz, 2007). However, it is important to highlight that there are interspecific overlaps in spectral acoustic parameters within the genus *Allobates* suggesting that sexual recognition and choice do not depend exclusively on acoustic signals, but also on the behavioral repertory, as visual and tactile signals (de Luna et al., 2010; Montanarin et al., 2011). New broad studies addressing such characteristics can shed more light on the connectivity of these *A. sumtuosus* populations.

Despite we detected a degree of genetic structure among *A. sumtuosus* populations, we found no evidence for its connection with their phenotypic variation. However, we detected a relationship between environmental changes and variation in genetic data, evidencing that the environment contributes to genetic changes in the studied populations, even if in a subtle way. Several studies have shown that the evolution of phenotypic and genotypic variation of single evolutionary entities with wide geographical distribution are often decoupled (Amézquita et al., 2009; Montanarin et al., 2011; Duarte et al., 2015). In some cases, the evolutionary diversification process is more easily perceived in one of these variation axes (genotypic vs. phenotypic), since phenotypic divergences is often more evident when selective pressures are studied at finer-scales (Rojas et al., 2019). The molecular marker used as a proxy for genetic variation (16S) has been widely reported as a good predictor of *Allobates* intraspecific and interspecfic diversification (Simões et al., 2014; Maia et al., 2017). However, we cannot rule out the possibility that the lower number of significant relationships of studied variables with the genetic variation be biased by the choice of the marker. The divergence in the mtDNA are known to be highly conservative in some cases and not neutral enough to investigate speciation (Galtier et al. 2009). Therefore, the divergence in the chosen marker may be disconnected from the detected phenotypic divergences in the interpopulational level we focused, which likely are under other selective pressures, and a denser genetic sampling would certainly increase the correspondence between the genotypic and phenotypic variation studied. However, even in a more subtle way, our results still indicate a role of the genetic divergence in the morphometric and acoustic differentiation within *A. sumtuosus*, which is also related to the latitudinal environmental gradient.

Conclusion

The latitudinal distance associated with the environmental distance likely shapes the acoustic characters of populations of *A. sumtuosus* by means of selective pressures on body size. This is because the latitudinal gradient crosses a climatic gradient, influencing changes to the area-volume relationship of individuals to maximize survival rates, and resulting in larger body sizes at warmer localities closer to the Equator. Consequently, the acoustic signals diverge together due to variations in the size of organs involved in vocalization. Despite showing the presence of an interpopulational genetic structure for the focal species, further studies with increased genetic information are needed to understand the causal effects of genetic variation found in these populations, as we detected that only the 16S gene variation was not associated with their phenotypic changes. Further studies on intersexual recognition also should help to understand the role of acoustic characteristics in the evolution of the focal species. In summary, this study breaks down the stages of speciation for this Amazonian litter-frog, demonstrating that environmental factors can lead to changes in sexual signals, through the variation in body size.

Acknowledgements We are grateful to the National Council for Scientific and Technological Development (CNPq) for the financial support through productivity grants to MM, IPF, APL and ILK; and a research grant (Universal 405640/2016-1) for MM. The Amazon Research Support Foundation (FAPEAM) for the master's scholarship to IYF. The Coordination for the Improvement of Higher Education Personnel (CAPES) for financial support and the Graduate Program in Ecology (PPG-Eco INPA) for structural and logistical support. Specimens were collected under collection permit 67501-2 provided by the Chico Mendes Institute for Biodiversity Conservation (ICMBio).

Compliance with Ethical Standards

Conflict of interest The author declares that he has no conflict of interest.

References

Aljanabi, S. M., & Martinez, I. (1997). Universal and rapid salt-extraction of high quality genomic DNA for PCR-based techniques. *Nucleic Acids Research, 25*(22), 4692–4693.

Amézquita, A., Flechas, S. V., Lima, A. P., et al. (2011). Acoustic interference and recognition space within a complex assemblage of dendrobatid frogs. *Proceedings of the National Academy of Sciences, 108*(41), 17058–17063.

Amézquita, A., Lima, A. P., Jehle, R., et al. (2009). Calls, colours, shape, and genes: A multi-trait approach to the study of geographic variation in the Amazonian frog *Allobates femoralis*. *Biological Journal of the Linnean Society, 98*(4), 826–838.

Barrett, J. C., Fry, B., Maller, J. D., et al. (2005). Haploview: Analysis and visualization of LD and haplotype maps. *Bioinformatics, 21*(2), 263–265.

Beebee, T. J. C. (2005). Conservation genetics of amphibians. *Heredity, 95*(6), 423–427.

Bevier, C. R., Gomes, F. R., & Navas, C. A. (2008). Variation in call structure and calling behavior in treefrogs of the genus *Scinax*. *South American Journal of Herpetology, 3*(3), 196–206.

Boul, K. E., Chris Funk, W., Darst, C. R., et al. (2007). Sexual selection drives speciation in an Amazonian frog. *Proceedings of the Royal Society B: Biological Sciences, 274*(1608), 399–406.

Charif, R. A., Waack, A. M., & Strickman, L. M. (2010). *Raven pro 1.4 user's manual* (p. 25506974). Ithaca, NY: Cornell Lab of Ornithology.

Chu, C., Lutz, J. A., Král, K., et al. (2019). Os efeitos diretos e indiretos do clima sobre a riqueza impulsionam o gradiente de diversidade latitudinal nas árvores da floresta. *Ecology Letters, 22*(2), 245–255.

Corander, J., & Marttinen, P. (2006). Bayesian identification of admixture events using multilocus molecular markers. *Molecular Ecology, 15*(10), 2833–2843.

Corander, J., Marttinen, P., Sirén, J., & Tang, J. (2008). Enhanced Bayesian modelling in BAPS software for learning genetic structures of populations. *BMC Bioinformatics, 9*(1), 539.

Cortázar-Chinarro, M., Lattenkamp, E. Z., Meyer-Lucht, Y., et al. (2017). Drift, selection, or migration? Processes affecting genetic differentiation and variation along a latitudinal gradient in an amphibian. *BMC Evolutionary Biology, 17*(1), 189.

Dal Vechio, F., Prates, I., Grazziotin, F. G., et al. (2018). Phylogeography and historical demography of the arboreal pit viper *Bothrops bilineatus* (Serpentes, Crotalinae) reveal multiple connections between Amazonian and Atlantic rain forests. *Journal of Biogeography, 45*(10), 2415–2426.

de Luna, A. G., Hödl, W., & Amezquita, A. (2010). Colour, size and movement as visual subcomponents in multimodal communication by the frog *Allobates femoralis*. *Animal Behaviour, 79*(3), 739–745.

De Queiroz, K. (2007). Species concepts and species delimitation. *Systematic Biology, 56*(6), 879–886.

Duarte, M. D. O., Freitas, T. M. D. S., & Prudente, A. L. D. C. (2015). Polychromatism of populations of *Corallus hortulanus* (Squamata: Boidae) from the southern Amazon Basin Brazil. *Acta Amazonica, 45*(4), 373–382.

Ernst, R., & Rödel, M. O. (2008). Patterns of community composition in two tropical tree frog assemblages: Separating spatial structure and environmental effects in disturbed and undisturbed forests. *Journal of Tropical Ecology, 24*(2), 111–120.

Erdtmann, L., & Amézquita, A. (2009). Differential evolution of advertisement call traits in dart-poison frogs (Anura: Dendrobatidae). *Ethology, 115*(9), 801–811.

Erdtmann, L., & Lima, A. P. (2013). Environmental effects on anuran call design: What we know and what we need to know. *Ethology Ecology & Evolution, 25*(1), 1–11.

Ferreira, A. S., Jehle, R., Stow, A. J., & Lima, A. P. (2018). Soil and forest structure predicts large-scale patterns of occurrence and local abundance of a widespread Amazonian frog. *Peer J, 6,* e5424.

Ferreira, A. S., Lima, A. P., Jehle, R., Ferrão, M., & Stow, A. (2020). The influence of environmental variation on the genetic structure of a poison frog distributed across continuous Amazonian rainforest. *Journal of Heredity, 111*(5), 457–470.

Ficetola, G. F., & Maiorano, L. (2016). Contrasting effects of temperature and precipitation change on amphibian phenology, abundance and performance. *Oecologia, 181*(3), 683–693.

Fouquet, A., Gilles, A., Vences, M., et al. (2007). Underestimation of species richness in neotropical frogs revealed by mtDNA analyses. *PLoS ONE, 2,* 1–10.

Gingras, B., Boeckle, M., Herbst, C. T., & Fitch, W. T. (2013). Call acoustics reflect body size across four clades of anurans. *Journal of Zoology, 289*(2), 143–150.

Hengl, T., de Jesus, J. M., MacMillan, R. A., et al. (2014). soilGrids1km—Global soil information based on automated mapping. *PLoS ONE, 9*(8), e105992.

Hijmans, R. J., Cameron, S. E., Parra, J. L., et al. (2005). Very high resolution interpolated climate surfaces for global land areas. *International Journal of Climatology, 25*(15), 1965–1978.

Hijmans, R. J., Van Etten, J., Cheng, J., et al. (2015). Package 'raster'. *R package*, 734.

Hoskin, C. J., James, S., & Grigg, G. C. (2009). Ecology and taxonomy-driven deviations in the frog call–body size relationship across the diverse Australian frog fauna. *Journal of Zoology, 278*(1), 36–41.

Hurvich, C. M., & Tsai, C. L. (1991). Bias of the corrected AIC criterion for underfitted regression and time series models. *Biometrika, 78*(3), 499–509.

Jaramillo, C., Rand, A. S., Ibáñez, R., & Dudley, R. (1997). Elastic structures in the vocalization apparatus of the tungara frog *Physalaemus pustulosus* (Leptodactylidae). *Journal of morphology, 233*(3), 287–295.

Jombart, T. (2008). adegenet: A R package for the multivariate analysis of genetic markers. *Bioinformatics, 24*(11), 1403–1405.

Jorge, R. F., Simões, P. I., Magnusson, W. E., & Lima, A. P. (2016). Fine-scale habitat heterogeneity explains the local distribution of two Amazonian frog species of concern for conservation. *Biotropica, 48*(5), 694–703.

Juncá, F. A. (1998). Reproductive biology of Colostethus stepheni and Colostethus marchesianus (Dendrobatidae), with the description of a new anuran mating behavior. *Herpetologica, 54,* 377–387.

Juo, A. S. R., & Franzluebbers, K. (2003). *Tropical soils: Properties and management for sustainable agriculture*. New York, NY: Oxford University Press.

Kaefer, I. L., & Lima, A. P. (2012). Sexual signals of the Amazonian frog *Allobates paleovarzensis*: Geographic variation and stereotypy of acoustic traits. *Behavior, 149*(1), 15–33.

Kaefer, I. L., Tsuji-Nishikido, B. M., Mota, E. P., et al. (2013). The early stages of speciation in Amazonian forest frogs: Phenotypic conservatism despite strong genetic structure. *Evolutionary Biology, 40*(2), 228–245.

Katoh, K., Rozewicki, J., & Yamada, K. D. (2019). MAFFT online service: Multiple sequence alignment, interactive sequence choice and visualization. *Briefings in Bioinformatics, 20*(4), 1160–1166.

Katoh, K., & Standley, D. M. (2013). MAFFT multiple sequence alignment software version 7: Improvements in performance and usability. *Molecular Biology and Evolution, 30*(4), 772–780.

Kearse, M., Moir, R., Wilson, A., et al. (2012). Geneious basic: An integrated and extendable desktop software platform for the organization and analysis of sequence data. *Bioinformatics, 28*(12), 1647–1649.

Keller, A., Rödel, M. O., Linsenmair, K. E., et al. (2009). The importance of environmental heterogeneity for species diversity and assemblage structure in Bornean stream frogs. *Journal of Animal Ecology, 78*(2), 305–314.

Kobayashi, S., Abe, S., Tomita, M., et al. (2018). Fine-scale genetic structure and estimation of gene flow of the Japanese brown frog *Rana japonica* in a Satoyama landscape on the western side of Inba Lake Eastern Japan. *Current Herpetology, 37*(1), 11–22.

Lampert, K. P., Rand, A. S., Mueller, U. G., et al. (2003). Fine-scale genetic pattern and evidence for sex-biased dispersal in the túngara frog *Physalaemus pustulosus*. *Molecular Ecology, 12*(12), 3325–3334.

Lanfear, R., Frandsen, P. B., Wright, A. M., et al. (2017). PartitionFinder 2: New methods for selecting partitioned models of evolution for molecular and morphological phylogenetic analyses. *Molecular Biology and Evolution, 34*(3), 772–773.

Leão-Pires, T. A., Luiz, A. M., & Sawaya, R. J. (2018). The complex roles of space and environment in structuring functional, taxonomic and phylogenetic beta diversity of frogs in the Atlantic Forest. *PLoS ONE, 13*(4), e0196066.

Liao, W., & Lu, X. (2012). Adult body size= f (initial size+ growth rate× age): Explaining the proximate cause of Bergman's cline in a toad along altitudinal gradients. *Evolutionary Ecology, 26*(3), 579–590.

Liberato, A. M., & Brito, J. I. B. (2010). Influência de mudanças climáticas no balanço hídrico da Amazônia Ocidental. *Revista Brasileira de Geografia Física, 3*(3), 170–180.

Liu, Q., Feng, H., Jin, L., et al. (2018). Latitudinal variation in body size in *Fejervarya limnocharis* supports the inverse of Bergmann's rule. *Animal Biology, 68*(2), 113–128.

Maia, G. F., Lima, A. P., & Kaefer, I. L. (2017). Not just the river: Genes, shapes, and sounds reveal population-structured diversification in the Amazonian frog *Allobates tapajos* (Dendrobatoidea). *Biological Journal of the Linnean Society, 121*(1), 95–108.

Maia-Carvalho, B., Vale, C. G., Sequeira, F., et al. (2018). The roles of allopatric fragmentation and niche divergence in intraspecific lineage diversification in the common midwife toad (*Alytes obstetricans*). *Journal of biogeography, 45*(9), 2146–2158.

Marchesini, A., Ficetola, G. F., Cornetti, L., et al. (2017). Fine-scale phylogeography of *Rana temporaria* (Anura: Ranidae) in a putative secondary contact zone in the southern Alps. *Biological Journal of the Linnean Society, 122*(4), 824–837.

Martin WF (1972) Evolution of vocalization in the genus *Bufo*. Evolution in the genus *Bufo*, pp 279–309

Menin, M., Lima, A. P., Magnusson, W. E., et al. (2007). Topographic and edaphic effects on the distribution of terrestrially reproducing anurans in Central Amazonia: Mesoscale spatial patterns. *Journal of Tropical Ecology, 23*(5), 539–547.

Mitchell, A., & Bergmann, P. J. (2016). Thermal and moisture habitat preferences do not maximize jumping performance in frogs. *Functional Ecology, 30*(5), 733–742.

Montanarin, A., Kaefer, I. L., & Lima, A. P. (2011). Courtship and mating behaviour of the brilliant-thighed frog *Allobates femoralis* from Central Amazonia: Implications for the study of a species complex. *Ethology Ecology & Evolution, 23*(2), 141–150.

Moraes, L. J. C. L., Pavan, D., Barros, M. C., & Ribas, C. C. (2016). The combined influence of riverine barriers and flooding gradients on biogeographical patterns for amphibians and squamates in south-eastern Amazonia. *Journal of Biogeography, 43*(11), 2113–2124.

Morales, V. (2002). Sistemática y biogeografía del grupo *trilineatus* (Amphibia, Anura, Dendrobatidae, *Colostethus*). *Publicaciones de La Asociacíon de Amigos de Doñana, 13,* 1–59.

Morales-Jimenez, A. L., Disotell, T., & Di Fiore, A. (2015). Revisiting the phylogenetic relationships, biogeography, and taxonomy of spider monkeys (genus *Ateles*) in light of new molecular data. *Molecular Phylogenetics and Evolution, 82,* 467–483.

Morton, E. S. (1975). Ecological sources of selection on avian sounds. *The American Naturalist, 109*(965), 17–34.

Mullen, L. M., Vignieri, S. N., Gore, J. A., et al. (2009). Adaptive basis of geographic variation: Genetic, phenotypic and environmental differences among beach mouse populations. *Proceedings of the Royal Society B: Biological Sciences, 276*(1674), 3809–3818.

Naka, L. N., & Brumfield, R. T. (2018). The dual role of Amazonian rivers in the generation and maintenance of avian diversity. *Science Advances, 4*(8), eaar8575.

Newman, R. A., & Squire, T. (2001). Microsatellite variation and fine-scale population structure in the wood frog (*Rana sylvatica*). *Molecular Ecology, 10*(5), 1087–1100.

Ng, J., Landeen, E. L., Logsdon, R. M., & Glor, R. E. (2013). Correlation between *Anolis* lizard dewlap phenotype and environmental variation indicates adaptive divergence of a signal important to sexual selection and species recognition. *Evolution International Journal of Organic Evolution, 67*(2), 573–582.

Ortiz, D. A., Lima, A. P., & Werneck, F. P. (2018). Environmental transition zone and rivers shape intraspecific population structure and genetic diversity of an Amazonian rain forest tree frog. *Evolutionary Ecology, 32*(4), 359–378.

Palumbi, S. R. (1996). Nucleic acids II: The polymerase chain reaction. In D. M. Hillis, C. Moritz, & B. K. Mable (Eds.), *Molecular Systematics* (pp. 205–247). Sunderland, MA: Sinauer & Associates Inc.

R Core Team (2019) R: A language and environment for statistical com- puting. R Foundation for Statistical Computing

Raffel, T. R., Rohr, J. R., Kiesecker, J. M., & Hudson, P. J. (2006). Negative effects of changing temperature on amphibian immunity under field conditions. *Functional Ecology, 20*(5), 819–828.

Rambaut, A., Drummond, A. J., Xie, D., et al. (2018). Posterior summarization in Bayesian phylogenetics using Tracer 1.7. *Systematic Biology, 67*(5), 901–904.

Ribas, C. C., Aleixo, A., Gubili, C., et al. (2018). Biogeography and diversification of *Rhegmatorhina* (Aves: Thamnophilidae): Implications for the evolution of Amazonian landscapes during the Quaternary. *Journal of Biogeography, 45*(4), 917–928.

Ribeiro, J. E. L. S., Hopkins, M. G., Vicentini, A., et al. (1999). *Flora da Reserva Ducke: Guia de Identificação das Plantas Vasculares* *de uma Floresta de Terra Firme na Amazônia Central*. Manaus: INPA.

Ronquist, F., Teslenko, M., Van Der Mark, P., et al. (2012). MrBayes 3.2: Efficient Bayesian phylogenetic inference and model choice across a large model space. *Systematic Biology, 61*(3), 539–542.

Rojas, D., Lima, A. P., Momigliano, P., et al. (2019). The evolution of polymorphism in the warning coloration of the Amazonian poison frog *Adelphobates galactonotus*. *Heredity, 124*(19), 1–18.

Rosseel, Y. (2012). Lavaan: An R package for structural equation modeling and more. Version 0.5–12 (BETA). *Journal of Statistical Software, 48*(2), 1–36.

Simões, P. I., Kaefer, I. L., Farias, I. P., & Lima, A. P. (2013). An integrative appraisal of the diagnosis and distribution of *Allobates sumtuosus* (Morales, 2002) (Anura, Aromobatidae). *Zootaxa, 3746*(3), 401–421.

Simões, P. I., & Lima, A. P. (2012). The tadpole of *Allobates sumtuosus* (Morales, '2000'2002) (Anura: Aromobatidae) from its type locality at Reserva Biológica do Rio Trombetas, Pará Brazil. *Zootaxa, 3499*(1), 86–88.

Simões, P. I., Stow, A., Hödl, W., et al. (2014). The value of including intraspecific measures of biodiversity in environmental impact surveys is highlighted by the Amazonian brilliant-thighed frog (*Allobates femoralis*). *Tropical Conservation Science, 7*(4), 811–828.

Spurgin, L. G., Illera, J. C., Jorgensen, T. H., et al. (2014). Genetic and phenotypic divergence in an island bird: Isolation by distance, by colonization or by adaptation? *Molecular Ecology, 23*(5), 1028–1039.

Stamatakis, A. (2014). RAxML version 8: A tool for phylogenetic analysis and post-analysis of large phylogenies. *Bioinformatics, 30*(9), 1312–1313.

Tryjanowski, P., Sparks, T., Rybacki, M., et al. (2006). Is body size of the water frog *Rana esculenta* complex responding to climate change? *Naturwissenschaften, 93*(3), 110–113.

Valenzuela-Sánchez, A., Cunningham, A. A., & Soto-Azat, C. (2015). Geographic body size variation in ectotherms: Effects of seasonality on an anuran from the southern temperate forest. *Frontiers in Zoology, 12*(1), 37.

van Rensburg AJ, Cortazar-Chinarro M, Laurila A et al (2018). Adaptive genomic variation associated with environmental gradients along a latitudinal cline in *Rana temporaria*. biorxiv 427872

Vences, M., Thomas, M., Van der Meijden, A., et al. (2005). Comparative performance of the 16S rRNA gene in DNA barcoding of amphibians. *Frontiers in Zoology, 2*(1), 5.

Zeisset, I., & Beebee, T. J. C. (2008). Amphibian phylogeography: A model for understanding historical aspects of species distributions. *Heredity, 101*(2), 109–119.

Zimmerman, B. L., & Bierregaard, R. (1986). Relevance of the equilibrium theory of island biogeography and species-area relations to conservation with a case from Amazonia. *Journal of Biogeography, 13*(2), 133–143.